Generation region of pulsating aurora obtained simultaneously by the FAST satellite and a Syowa-Iceland conjugate pair of observatories

N. Sato,[1,2] D. M. Wright,[3] C. W. Carlson,[4] Y. Ebihara,[1] M. Sato,[5,6] T. Saemundsson,[7] S. E. Milan,[3] and M. Lester[3]

Received 4 February 2004; revised 1 July 2004; accepted 26 July 2004; published 7 October 2004.

[1] We have carried out a direct comparison of pulsating auroras observed from the ground at Syowa Station in Antarctica and on board the FAST satellite (~3100 km altitude), with reference to simultaneous data obtained by a Syowa-Iceland conjugate pair of observatories. The aurora at Syowa appeared as east-west aligned bands consisting of two different types: a poleward moving oscillation and a standing oscillation, each with a period of ~6 s. Spatial and temporal variations of the downgoing high-energy (>5 keV) electron flux obtained by FAST showed a one-to-one correspondence with the optical pulsating aurora. The occurrence regions of the two different types of pulsating aurora were separated by a narrow gap (~7–10 km in width at 100 km altitude) in the inverted-V structure, and the gaps were colocated with the small-scale upward field-aligned currents. The time-varying magnetic fields (upward field-aligned current) observed by FAST were almost correlated (in-phase) with the downgoing electron flux (>5 keV) modulations. Both the optical emission intensity at Syowa and the downgoing high-energy electron flux (>7 keV) on board FAST showed ~3 Hz modulation. The ~3 Hz fine structure constituted the main body of the ~6 s pulsating aurora. VLF wave activities were not observed by FAST in the region of pulsating aurora. The source regions of the generation or modulation of the energetic particles are estimated to be at a higher altitude than FAST, in the region of ~2 Re to 6 Re from the satellite. This suggests that the source region is not located in the equatorial plane of the magnetosphere but is located earthward, far from the equatorial plane. The conjugate pair observations on the ground revealed that the aurora, though pulsating in both hemispheres, was not conjugate in shape, appearing as an east-west aligned band in the Southern Hemisphere but as a torch structure (omega band) in the Northern Hemisphere. The evidence presented in this study suggests that ionosphere-magnetosphere coupling processes are important in producing the pulsating aurora. *INDEX TERMS:* 2704 Magnetospheric Physics: Auroral phenomena (2407); 2736 Magnetospheric Physics: Magnetosphere/ionosphere interactions; 2740 Magnetospheric Physics: Magnetospheric configuration and dynamics; 2716 Magnetospheric Physics: Energetic particles, precipitating; *KEYWORDS:* aurora, pulsating aurora, conjugacy, Antarctica

Citation: Sato, N., D. M. Wright, C. W. Carlson, Y. Ebihara, M. Sato, T. Saemundsson, S. Milan, and M. Lester (2004), Generation region of pulsating aurora obtained simultaneously by the FAST satellite and a Syowa-Iceland conjugate pair of observatories, *J. Geophys. Res.*, *109*, A10201, doi:10.1029/2004JA010419.

1. Introduction

[2] Pulsating auroras are common phenomena, which are observed universally during the recovery phase of substorms in the auroral and subauroral zones. Most of the known characteristics of pulsating auroras have been reviewed by *Johnstone* [1983], *Davidson* [1990], and *Nemzek et al.* [1995]. Here we briefly summarize the basic qualities of the pulsating auroras, which may relate to this study. They exhibit typical periods of a few seconds to a few tens of seconds. Rapid ~3 Hz modulations are often observed in the pulsation structure [e.g., *Royrvik and Davis*, 1977; *Sandahl et al.*, 1980; *Winckler and Nemzek*, 1993]. Usually, pulsating auroras manifest themselves inside an individual luminous patch of irregular shape,

[1]National Institute of Polar Research, Tokyo, Japan.
[2]Also at Department of Polar Science, Graduate University for Advanced Studies, Tokyo, Japan.
[3]Department of Physics and Astronomy, University of Leicester, Leicester, UK.
[4]Space Science Laboratory, University of California, Berkeley, California, USA.
[5]Department of Geophysics, Tohoku University, Sendai, Japan.
[6]Now at Institute of Physical and Chemical Research (RIKEN), Wako, Japan.
[7]Science Institute, University of Iceland, Reykjavik, Iceland.

0148-0227/04/2004JA010419$09.00

with similar dimensions in both latitude and longitude. Typical scale sizes are 10–200 km [*Harang*, 1951; *Oguti*, 1978; *Yamamoto*, 1988]. Sometimes, though, the structures greatly elongate several hundred kilometers in longitude. Rocket measurements have demonstrated that modulated electron fluxes from as low as a few keV to 100 keV are responsible for these phenomena [e.g., *Sandahl et al.*, 1980; *McEwen et al.*, 1981].

[3] The most widely held theoretical view (hereinafter called the classical/standard model) of pulsating aurora generation envisages a type of relaxation oscillator involving trapped electrons and VLF wave-producing instabilities in the equatorial plane of the magnetosphere. The shape of each luminous patch in the ionosphere represents the magnetic mapping of a region of enhanced plasma density near the equatorial plane [*Trakhtengerts et al.*, 1986; *Davidson*, 1990; *Demekhov and Trakhtengerts*, 1994]. One of the most important considerations for theories of pulsating aurora is the location of the interaction, which generates the electron precipitation. The bulk of the available evidence indicates a source far out in the magnetosphere, probably near the equatorial plane. This conclusion relies on two primary sources of information: observations of pulsating auroral displays showing close conjugacy [*Stenbaek-Nielsen et al.*, 1972] and analysis of the energy dispersion presented in precipitation pulses measured at rocket altitude [*Bryant et al.*, 1975; *Lepine et al.*, 1980; *Yau et al.*, 1981].

[4] On the other hand, *Stenbaek-Nielsen* [1980] has proposed that active ionospheric processes probably play an important role in causing or modifying pulsating auroras. *Sato et al.* [1998a] found some supporting evidence for the active role of the ionosphere based on nonconjugate features of pulsating auroras relating to their shapes and periodicities. *Tagirov et al.* [1999] discussed a new approach including the effects of relaxation characteristics of the ionosphere. They suggested that the relaxation time of the ionosphere should be reflected in the pulsation periods.

[5] However, even today, there is no direct evidence to support the classical/standard model, as regards the generation region, periodicity, and shapes. This is because of a lack of direct satellite observations of pulsating auroral patches in the source/modulation regions. In general, spacecraft observations of these phenomena have not been able to distinguish between their spatial and temporal characteristics because of the complex shapes, rapid movements, and periodicities exhibited by pulsating auroras. For an investigation of the generation region and modulation mechanism for pulsating aurora, simultaneous observations of optical aurora from conjugate observatories on the ground and from satellites are very important. The Fast Auroral Snapshot (FAST) satellite was specifically designed to investigate the plasma physics of auroral phenomena at very high resolution in time and space within the acceleration regions [e.g., *Carlson et al.*, 1998]. Recently, *Sato et al.* [2002] reported a preliminary result of the direct comparison of pulsating aurora observed simultaneously by the FAST satellite and from the ground at Syowa Station in Antarctica ($L \sim 6.4$). The major findings in their study are that (1) spatial and temporal variations of the downgoing, high-energy (>5 keV) electron flux showed a one-to-one correspondence with the optical pulsating aurora, (2) pulsating auroras occurred within the region of the inverted-V structure of lower-energy (0.1–1 keV) electron precipitation, (3) the occurrence regions of the two different types of pulsating aurora, poleward moving and standing oscillation, were clearly separated by the narrow gap in the inverted-V structure, (4) the downgoing high-energy ion flux modulation was almost out of phase (anticorrelated) with the downgoing high-energy electron flux modulation. They proposed that the precipitating high-energy electrons, which produce the pulsating aurora, are modulated by the oscillation of the field-aligned electric field located above the FAST satellite. Such studies provide important evidence regarding the generation mechanism of pulsating aurora.

[6] The study presented in this paper is an extension of the work of *Sato et al.* [2002] focusing on the modulation/generation region of pulsating aurora using high time resolution data sets obtained simultaneously from the FAST satellite and from the ground at Syowa Station. We will also examine the geomagnetically conjugate characteristics of this event as recorded by TV cameras at a Syowa-Iceland conjugate pair of observatories. A primary conclusion of this study is that the shape of the pulsating aurora showed nonconjugacy and that the generation/modulation region could not have been located in the equatorial plane of the magnetosphere but was probably somewhere between the equatorial plane and FAST. Finally, we will propose a schematic model to explain this event.

2. Observations

[7] At Syowa Station in Antarctica, a white-light all-sky TV camera recording at 30 frames/s and a digital white-light all-sky camera (ASC) recording at 20 s/frame with a 2-s exposure time were in operation on 30 September 2000 during the Syowa-Iceland conjugate auroral campaign. The geographic and geomagnetic coordinates of the conjugate pair are 69.00°S, 39.58°E (INV. LAT: 66.6°, MLON: 71.8°, L-value: 6.35; MLT: UT + 15 min) for Syowa, and 66.42°N, 15.93°W (INV. LAT: 66.8°, MLON: 72.9°, L-value: 6.44; MLT: UT + 23 min) for Raufarhofn in Iceland. At Raufarhofn the same type of all-sky TV camera as at Syowa was in operation. An auroral breakup occurred at ~2246 UT at lower latitudes relative to the Syowa/Iceland observatories and the active auroral region expanded rapidly poleward. Afterward, the breakup aurora was replaced by a new pulsating aurora at ~2312 UT at the conjugate pair of observatories during the recovery phase of the substorm. The FAST satellite passed over the field of view of the Syowa all-sky camera from ~2318 UT to ~2321 UT when the pulsating aurora was observed. The altitude of FAST was ~3100 km.

2.1. Direct Comparison of ~6 s Pulsating Aurora Obtained From the FAST Satellite and on the Ground at Syowa

[8] *Sato et al.* [2002] has reported a preliminary survey of the pulsating auroral event of 30 September 2000. As an aid to understanding this event, we will discuss briefly certain basic features before investigating new findings regarding ~6 s pulsating auroras. The top left panel of Figure 1 shows an ASC snapshot image at 2318:31 UT. The footprint of FAST mapped to 100-km altitude is

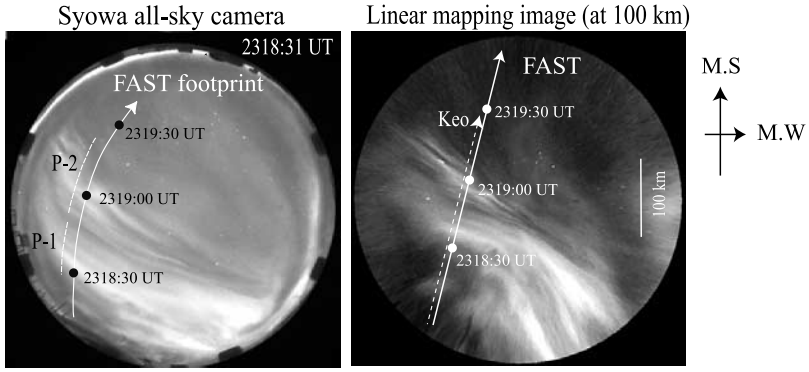

Figure 1. The left panel shows a white-light snapshot image from the Syowa all-sky camera at 2318:31 UT. The footprint of FAST mapped to 100-km altitude is marked in this image. The top right panel shows the same auroral image remapped at 100 km altitude with a linear scale from the original image. Both images were reversely remapped in the east-west direction relative to the original all-sky images.

marked in this ASC image. The top right panel of Figure 1 shows the auroral image remapped at 100 km altitude with a linear scale from the all-sky image. It should be noted that the east-west directions in Figure 1 have been remapped in reverse relative to the original all-sky images in order to correspond to the directions in the images obtained in the Northern Hemisphere. The Keogram along the FAST footprint, which is shown in the top panel of Figure 2, was generated from the linear scale TV image data. We shall begin by describing some distinctive features of the optical pulsating aurora that appear in the ASC image and the Keogram. The auroral image shows that the pulsating aurora consists of multiple east-west aligned bands. Furthermore, there are two different types of pulsating aurora (pulsation 1 (P-1) and pulsation 2 (P-2)). Pulsation 1 is the poleward moving form located at lower latitudes, while pulsation 2 is the standing form located at higher latitudes, relatively speaking. The recurrence period is ~6 s for both types of pulsation. The FAST footprint and Keogram indicate that FAST entered the region of P-1 at ~2318:28 UT and exited from the region of P-2 at ~2319:08 UT. The second panel of Figure 2 illustrates the energy-time spectrum of downgoing electrons obtained by the FAST satellite. The energy spectrum demonstrates that accelerated electron flux enhancements forming inverted-V structures (marked as black dotted lines) are observed in the energy range of ~0.1–1 keV during the intervals from "A" to "F." Brief, spatially narrow "gaps" in the inverted-V structure are found during the intervals "B-C" and "D-E." The scale size for the gaps of "B-C" and "D-E" is ~10 km and ~7 km at 100 km altitude. A higher-energy flux modulation is observed for electron energies of more than a few keV (marked by a white, dotted line on the energy spectrum), and this is well correlated with the temporal and spatial variations of the optical pulsating aurora. However, the lower-energy (0.1–1 keV) flux modulation, which is forming the inverted-V structure, does not show such a clear relationship with the optical pulsating aurora. The temporal and spatial variation of the total energy flux of downgoing electrons for >5 keV is plotted with a black dotted line on to the Keogram of the top panel of Figure 2. It can clearly be seen that the optical pulsation "ON-OFF" cycle shows a one-to-one correlation with the high-energy electron flux variations. New features of the ~6 s optical and electron pulsating auroras, which *Sato et al.* [2002] did not report, are indicated by the area delineated by the white dotted line, which is lower in region P-2 than in region P-1 (by 5–8 keV), contrary to the behavior of the inverted-V feature. Furthermore, the white dotted line in region P-2 looks like an extension of the inverted-V feature, although region P-1 is independent of that feature. It is difficult to find any definite energy peak, which might represent equipotential acceleration, within the white dotted lines of both regions P-1 and P-2. It is also found that after the gap "D-E" in the spectrogram/Keogram (top two panels of Figure 2), the inverted-V structure appears to continue, although the >5 keV flux is diminished, and FAST is outside of region P-2. We will discuss these features later.

[9] We shall now examine the relationship among the downgoing electrons, ions, and field-aligned currents obtained by FAST. The third panel of Figure 2 shows the energy-time spectra of the downgoing ions. The bottom panel of Figure 2 shows the eastward component of the magnetic field. It is found from the energy-time spectrum of downgoing ions that an ion-flux enhancement in the energy range of ~0.2–0.8 keV is observed during the interval before ~2318:30 UT. Afterward, this ion flux suddenly decreases until the end of the interval in this panel. On the other hand, another ion-flux enhancement is seen in the energy range of ~1–5 keV throughout the whole interval. It is evident from the second and bottom panels of Figure 2 that the regions of inverted-V structures correspond to those of upward field-aligned currents, if we assume that sheet-type field-aligned currents are present along the east-west direction. This characteristic suggests that the upward field-aligned currents are dominantly driven by the downgoing low-energy electrons, which form inverted-V structures. Though the occurrence regions of P-1 and P-2 correspond to those of upward field-aligned currents, these currents may not be a sufficient condition to generate pulsating aurora. An example of this is seen in the space between "E" and "F," where there is an upward field-aligned current but no auroral pulsation. The region of lower ion flux in the energy range of 0.1–1 keV corresponds to a region of downward field-aligned current. It is also apparent that the region of sudden decrease of this ion flux at

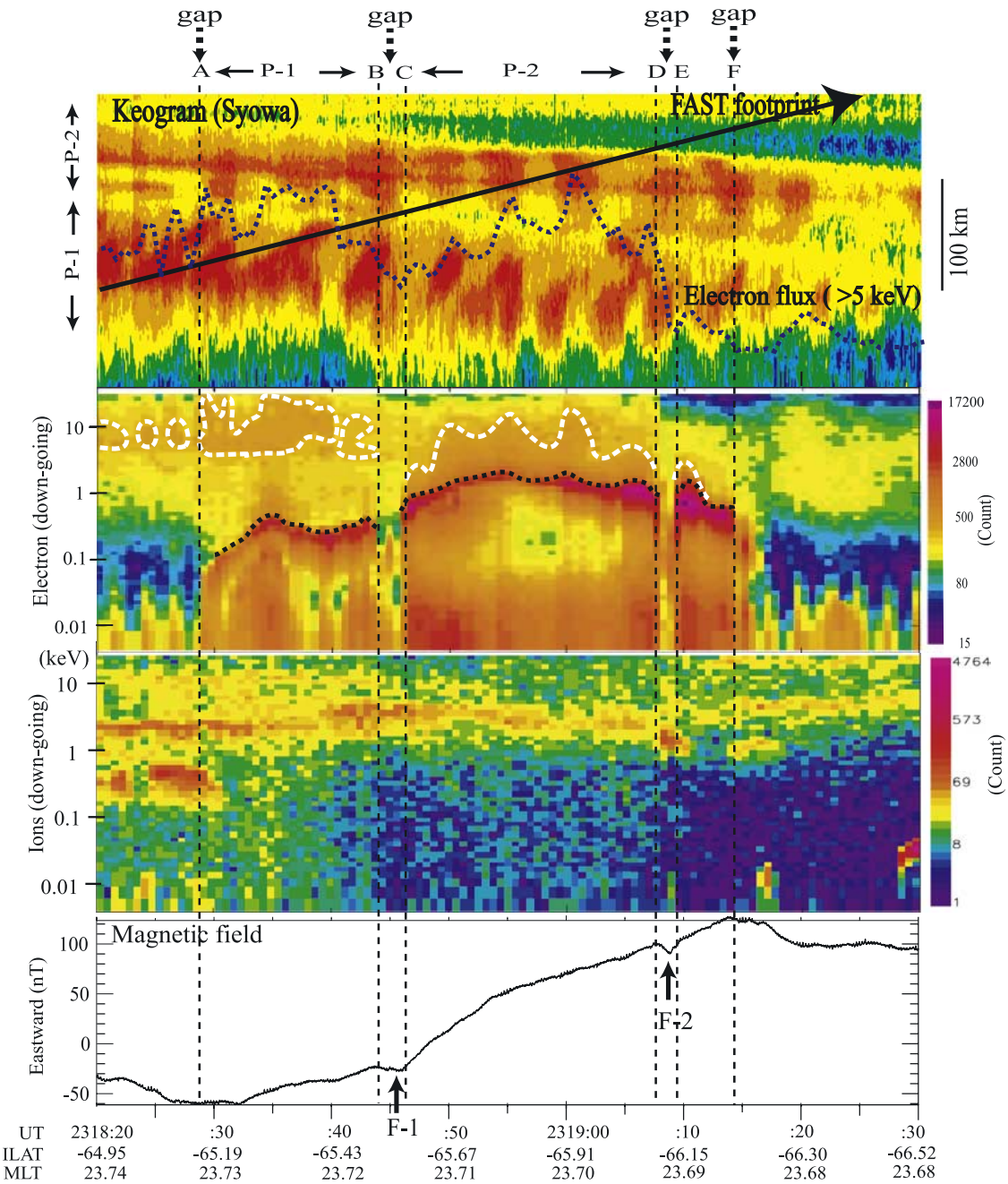

Figure 2. The top panel presents the Keogram reproduced from the Syowa all-sky TV camera data along the FAST footprint, together with the total energy flux variations of downgoing electrons for >5 keV obtained by FAST. The energy spectrum of the downgoing electrons and the down-going ions are illustrated in the second and the third panels. The eastward component of the magnetic field is shown in the bottom panel, where ILAT and MLT stand for invariant latitude and magnetic local time, respectively.

~2318:30 UT corresponds to the region where the direction of the field-aligned current turns from downward to upward. On the other hand, the ion fluxes in the energy range of ~1–10 keV show a clear, isolated ion-flux enhancement in the region of the spatially narrow "gap" of "D-E" in the inverted-V structure. Furthermore, it is worth noting that the "gaps" of the inverted-V structure, "B-C" and "D-E," are colocated with the small-scale field-aligned currents, marked with arrows "F1" and "F2" in the bottom panel of Figure 2. The feature "F2" is a magnetic negative bay, which suggests that a small-scale downward field-aligned current exists there. "F1" is a similar but weaker negative bay. We can explain why the "gaps" of the inverted-V structure are located at "F1" and "F2" and why the higher ion fluxes show a clear isolated enhancement in the region of "F2" if we assume that the small-scale downward field-aligned currents are directly associated with the field-aligned electric field.

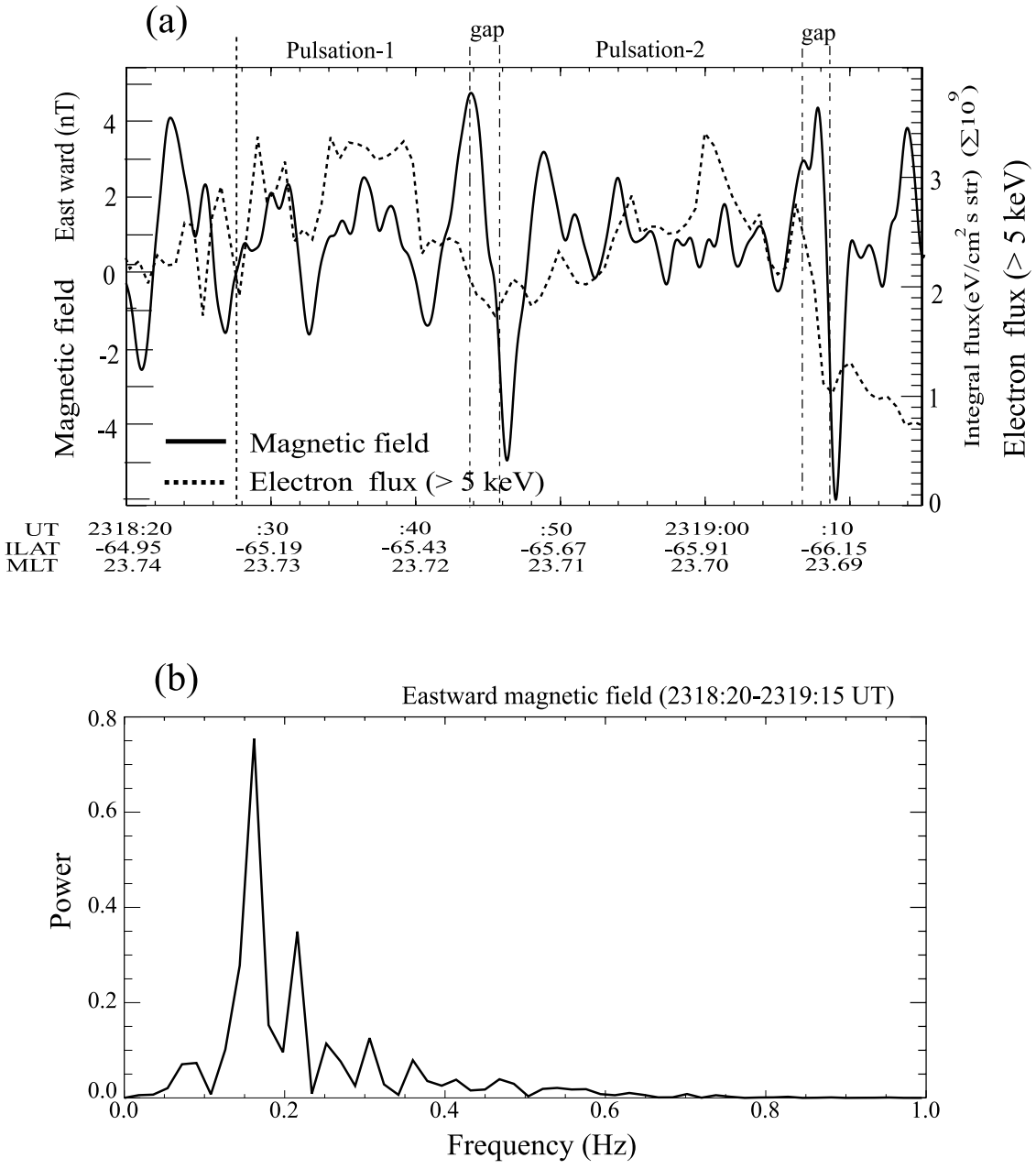

Figure 3. (a) The solid line shows the eastward component of magnetic field filtered to exclude periods outside in the range 0.9–9 s (0.11–1.11 Hz pass band) and the dotted line shows the downgoing electron flux (>5 keV) in the interval of 2318:20–2319:15 UT obtained by FAST. (b) A power spectrum of the magnetic field variation calculated by the FFT spectral analysis method during the interval shown in Figure 3a.

[10] The solid line of Figure 3a shows the eastward component of magnetic field filtered to exclude periods outside in the range 0.9–9 s (0.11–1.11 Hz pass band) and the dotted line shows the downgoing electron flux (>5 keV) in the interval of 2318:20–2319:15 UT obtained by FAST. It is seen that the magnetic field variations are almost correlated (in-phase) with the downgoing electron flux (>5 keV) variations especially during the interval of ~2318:27 UT and 2318:44 UT in the region of pulsation 1. The in-phase relationship suggests that the downgoing high-energy electrons that are responsible for producing the optical pulsation correlate with the time-varying upward field-aligned current. Figure 3b shows the power spectrum of the filtered magnetic field variation obtained by the FFT spectral analysis method during the interval shown in Figure 3a. A clear spectral peak is found at ~0.16 Hz (~6 s), which is almost the same period as the optical pulsation.

[11] The field-aligned electric field intensity (not shown) observed by FAST is rather weak and stable (from zero to less than −10 mV/m) in both the P-1 and P-2 regions. These features suggest that the acceleration region may be located far from the FAST spacecraft in altitude.

2.2. High-Frequency ~3 Hz Pulsation on the Ground and on Board FAST

[12] Pulsating auroras often exhibit ~3 Hz modulation, as documented in section 1. Here we will examine the features associated with such modulations using TV camera data from the ground at Syowa and the downgoing electrons on board the FAST satellite.

[13] The top left panel of Figure 4 shows again the all-sky snapshot from Figure 1. The top right panel shows a spatially expanded display of the area marked with a white rectangle in the left panel. R-0, R-1, R-2, R-3, and R-4 show the regions for which we have reproduced a temporal luminosity variation from the all-sky TV camera data. The area of box R-0 is ~220 km^2, and the distance between the center of R-0 and other box centers is ~15 km at 100 km altitude. However, it is difficult to establish the exact scale size because the real scale depends on auroral altitude and elevation angle in the all-sky images. The direction between R-1 and R-2 and between R-3 and R-4 closely follows the east-west aligned pulsating aurora. The region R-0 is located centrally. The middle panel of Figure 4 shows the luminosity variations of the pulsating aurora in all five regions during the interval from 2318:20 to 2319:00 UT. The bottom panel of Figure 4 resembles the middle panel except for the reduced time interval of 2318:34 UT to 2318:41 UT. It can be seen that the ~6 s intensity oscillations exhibit submodulations at ~3 Hz. Though it is difficult to show a correlation in intensity variations between boxes during the whole interval, in this shorter interval a definite correlation was found between R1 and R2 and also between R-3 and R-4. This suggests that the ~3 Hz auroral oscillation is aligned east-west rather than north-south. It follows that the ~3 Hz modulation shows less tendency for poleward motion. In other words, the ~3 Hz pulsation occurs along the main body of an east-west aligned auroral form pulsating at ~6 s, but the filament of each east-west aligned pulsating aurora is narrow in comparison with the main body of ~6 s pulsating aurora.

[14] Figure 5 shows higher time resolution data of the flux variations of the downgoing electrons in the energy ranges of 20 keV, 14 keV, 10 keV, 7 keV, and 5 keV, observed by FAST. The top panel covers the period 2318:19 to 2318:51, while in the middle and bottom panels the timescale has been expanded for the intervals ~2318:34 to 2318:41 and 2318:34 to 2318:38 UT. It is clear that there are ~3 Hz modulations of the electron precipitation, especially at energies greater than 5 keV. The ~3 Hz signatures are energy-dispersed, appearing first at higher energies. This effect can be explained by the finite travel time of the electrons from the source region. If we assume that modulation is simultaneous at all energies and that particles travel with constant speed after modulation, we can estimate a distance from the source (or modulation region) of the ~3 Hz modulated electrons, applying the method previously employed in rocket observations [*Bryant et al.*, 1975; *Lepine et al.*, 1980; *Yau et al.*, 1981] and FAST satellite observations [*Cash et al.*, 2002]. Figure 6a shows the inverse velocity of the five phase profiles, A ~ E and A′ ~ E′ marked on the bottom panel of Figure 4 to identify the best one-to-one correspondence of the flux variations in the different energy ranges. The solid lines of A ~ E represent the fitting plots for all four energy ranges, and the dotted lines of A′ ~ E′ represent the fitting plots between the two energy ranges of 20 keV and 14 keV. The significance of the dotted lines is that the higher-energy electrons may contribute more to the optical emission intensity than lower-energy electrons do, and the pulses from 20 keV to 14 keV are significantly different from other pulses in Figure 5. Assuming that the electrons are field-aligned (downgoing electrons having a pitch angle of 180° in the Southern Hemisphere), the calculated distances for the pulsations A, B, C, D, and E between the source region and the FAST satellite along a magnetic field line are ~4.9 Re, ~6.2 Re, ~6.1 Re, ~3.8 Re, and ~3.9 Re for solid line and ~2.2 Re, ~3.6 Re, ~2.4 Re, ~3.2 Re, and ~2.5 Re for dotted line, respectively. The results show that the source region calculated for the two energy ranges (20 keV and 14 keV) is located further earthward and is less scattering than that calculated for all energy ranges. The uncertainty in the distance calculations caused by the ambiguity of the fitting lines (solid lines) of A ~ E is roughly 0.5 Re. Figure 6b shows the source position mapped onto the latest model magnetospheres: T01_01 [*Tsyganenko*, 2002a, 2002b] and T01_S (storm time model) [*Tsyganenko et al.*, 2003]. The solar wind parameters obtained by the ACE satellite, together with the Dst index, are shown in the model magnetosphere. These plots show that the generation regions of the ~3 Hz particle modulation are scattered over a distance ranging between 2.2 Re and 6.2 Re from FAST along the field line. It is very important to note here that the source/modulation region is far from the equatorial plane of the magnetosphere, regardless of the time interval and magnetospheric model.

[15] It is also important to consider the source region of the ~6 s pulsation envelope. The middle panel of Figure 5 shows almost one cycle of ~6 s pulsation in the "ON" phase. The pulsation "OFF" phase started at ~2318:40 UT, marked with an arrow in this figure. It is clear that the "OFF" signature is energy-dispersed, with almost the same time lag as the ~3 Hz modulation shown in the bottom panel of Figure 5. This suggests that the ~6 s pulsation envelope could have its origin in the ~3 Hz modulation region, far from the equatorial plane of the magnetosphere. These results cast doubt on the classical/standard models, which are based on the simple assumption that the generation/modulation region is located at or in the vicinity of the equatorial plane of the closed magnetosphere, as outlined in section 1. We will discuss this issue later.

2.3. Conjugacy of Pulsating Aurora Obtained by the Syowa-Iceland Conjugate Pair

[16] Syowa Station in Antarctica and Raufarhofn in Iceland form an ideal pair of observatories for studying geomagnetically conjugate optical auroras. The geomagnetic conjugate point of Syowa at 2320 UT on 30 September 2000 as calculated by the IGRF model is located at 66.1°N and 17.3°W, only ~70 km from Raufarhofn. It is common knowledge that the exact location of the conjugate point varies with magnetic activity and IMF parameters. The auroral event in this study occurred under disturbed conditions, $Kp = 6_+$. We have calculated the conjugate point of Syowa using the latest magnetic field models, T01_01 [*Tsyganenko*, 2002a, 2002b] and T01_S [*Tsyganenko et al.*, 2003], also used in Figure 6. Figure 7 shows the fields of view

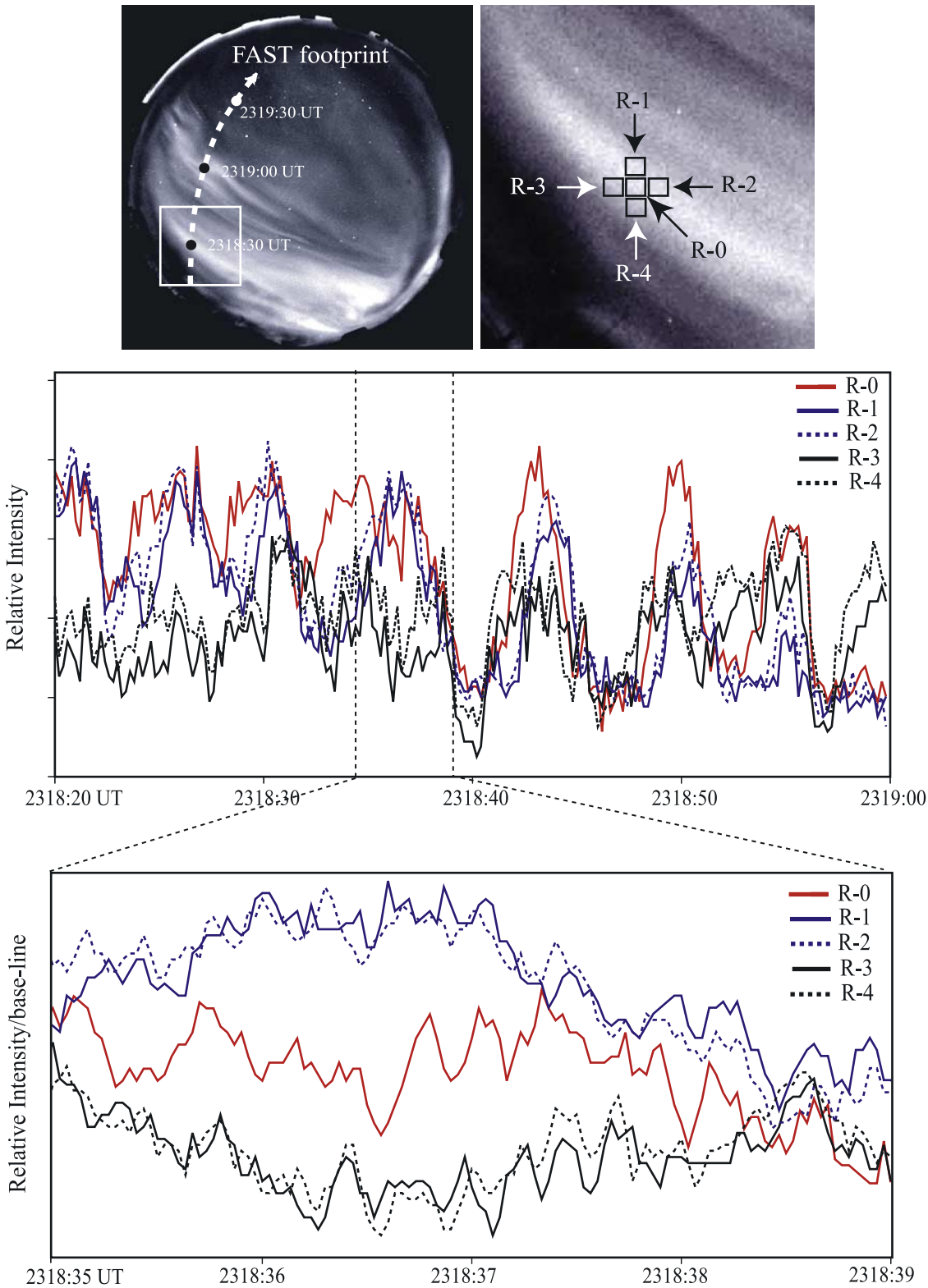

Figure 4. The top left panel shows a snapshot of the all-sky auroral image. The top right panel shows a spatially expanded display from the original all-sky image of the area marked with a white rectangle in the left panel. The middle panel indicates the luminosity variations of the pulsating aurora detected in the regions R-0, R-1, R-2, R-3, and R-4. The bottom panel shows the same display as the middle panel for a more restricted time interval. It is found that ~3 Hz intensity modulations are superimposed on the ~6 s pulsating auroras in all five regions.

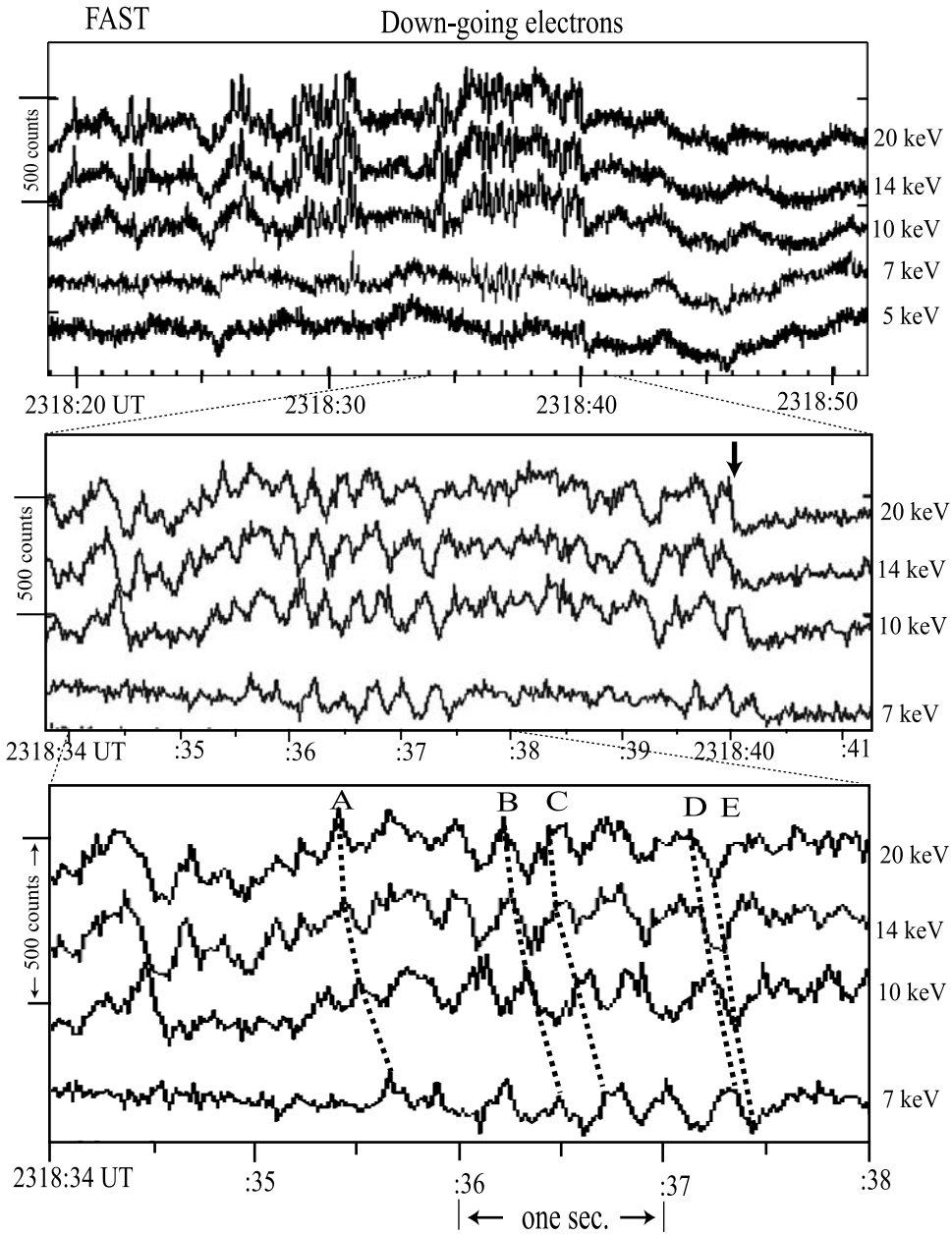

Figure 5. The top panel shows higher time resolution data of the flux variations of the downgoing electrons in the energy ranges of 20 keV, 14 keV, 10 keV, 7 keV, and 5 keV observed by FAST. The middle and bottom panels give identical information for more restricted intervals. It is clear that the electron precipitation shows a ~3 Hz modulation and that it exhibits energy-time dispersion.

of the all-sky TV camera at Raufarhofn and at the calculated conjugate points of Syowa, assuming a 470 km radius at 100 km altitude, where the radius of 470 km corresponds to the effective observational zenith angle of 80° for the all-sky camera [*Minatoya et al.*, 1994]. It is obvious that the all-sky field of view of Raufarhofn coincides with the calculated conjugate fields of view, more or less, even if the actual conjugate point is based on T01_S.

[17] The top two panels of Figure 8 show snapshot images from the conjugate pair of all-sky cameras obtained at 2318:51 UT, 2319:57 UT, 2320:34 UT, and 2321:03 UT. The directions of magnetic poleward and east-west are the same at the conjugate auroral images as was the case in Figure 1. The form of aurora over Iceland can be classified as a "torch structure" [*Royrvik and Davis*, 1977; *Oguti et al.*, 1981]. Over Syowa, however, the aurora appeared as an east-west aligned band at 2318:51 UT. Torch-structure type aurora has been shown to be identical to "omega band" aurora [*Oguti et al.*, 1981] and generally occurs in the midnight and early morning sector during magnetically active periods. The torch structure aurora observed over Iceland showed pulsations with a period of ~6 s, as seen in the bottom two panels of Figure 8. One could say therefore that conjugacy was established in the sense that similar

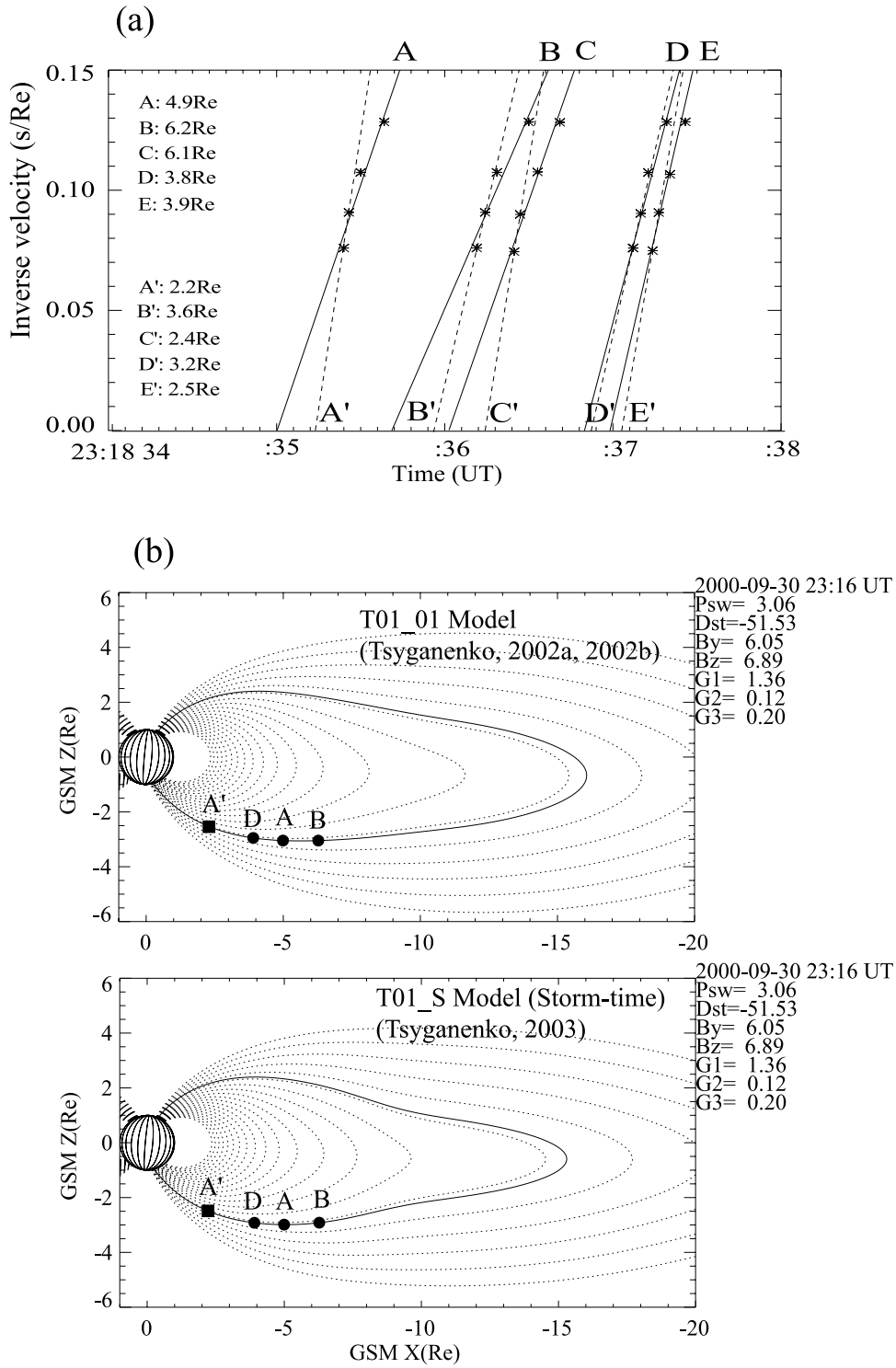

Figure 6. (a) The inverse velocity at five different times/positions marked on the bottom panel of Figure 5. The solid lines of A ∼ E represent the fitting plots for all four energy ranges, and the dotted lines of A′ ∼ E′ represent the fitting plots between the two energy ranges of 20 keV and 14 keV. The calculated distance between the source region and the FAST satellite at each interval is shown in this figure. (b) The calculated source positions are mapped onto the latest model magnetospheres, T01_01 and T01_S.

pulsations appeared in both hemispheres, but this conjugacy was not reflected in the large-scale structure of the aurora. It is interesting, however, to examine the temporal and spatial developments of the pulsating aurora at the conjugate pair of observatories. Interhemispheric discrepancies are apparent, the bands at Syowa developing actively toward a torch structure from the second left panel (2319:57 UT) to the last panel (2321:03 UT), while the torch structure in the

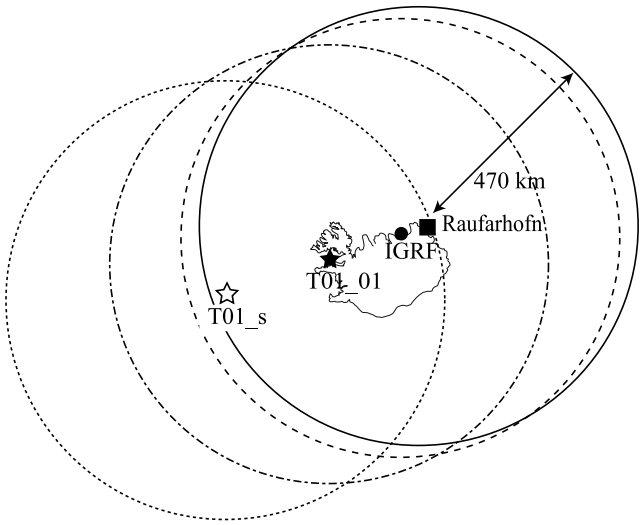

Figure 7. The geomagnetic conjugate point of Syowa at 2320 UT on 30 September 2000, calculated by the geomagnetic field models of IGRF, T01_01 and T01_S, are plotted on a map of Iceland. The field of view of all-sky TV camera at Raufarhofn and the calculated conjugate of the field of view of the Syowa camera are also plotted in this figure, assuming a radius of 470 km at 100 km altitude.

Northern Hemisphere remains stable. It is important to note here that the auroral features visible from Syowa become more active with time within the field of view. This suggests that the torch structure developing at Syowa is not the result of a drift of the occurrence region into the all-sky field of view of Syowa but rather that the auroras are caused by the activation of the auroral luminosity within the field of view. It is also clear that the overall form of the aurora is different in the two hemispheres. We have to note here that the auroral structure in the far north and/or northwest of the Iceland all-sky images (Figures 8b, 8c, and 8d) is a discrete auroral not the conjugate representation of the Syowa torch. These facts suggest that the nonconjugate shapes of the aurora were not caused by a displacement of the conjugate field lines but resulted from an asymmetry in the generation conditions in the two hemispheres.

[18] The middle two panels and the bottom two panels of Figure 8 show the conjugate Keograms reproduced from the all-sky TV camera data in the geomagnetic north-south and its orthogonal (nearly geomagnetic east-west) directions, respectively. The positions and the directions for each Keogram are marked on the snapshot displays of all-sky images as seen in the top left panel of Figure 8. The vertical dotted lines in the Keograms show the positions of the snapshot auroral images displayed at the top panel of this figure. The Keograms show that the east-west aligned pulsating aurora observed at Syowa during the interval of ~2316–2321 UT drifts equatorward and eastward. The torch structure pulsating aurora observed at Raufarhofn in Iceland during the interval of ~2317–2323 UT also drifts equatorward but there is no clear eastward drift. The pulsating torch structure apparent at Syowa from ~2320 UT does not show any obvious drift. This torch structure starts developing when the activity of the torch structure in Iceland is decreasing. In other words, this torch structure pulsating aurora was not conjugate in either shape or dynamics.

3. Summary and Discussion

[19] We have carried out a direct comparison of pulsating auroras observed from the ground at Syowa in Antarctica and on board the FAST satellite together with conjugate pair observations on the ground at the Syowa and Iceland observatories. Combining high-resolution measurements made by the FAST satellite with simultaneous conjugate optical observations on the ground, we were able to resolve spatial and temporal ambiguities associated with the observed pulsating auroral phenomena. The major findings of this study are as follows.

[20] 1. The magnetic field variations obtained by FAST were almost correlated (in-phase) with the downgoing electron flux (>5 keV) modulations, especially in the region of pulsation 1.

[21] 2. The downgoing ion flux enhancement in the moderate energy range 0.1–1 keV corresponded to region of the downward field-aligned current. The ion flux in this energy range decreased suddenly in the region of upward field-aligned current.

[22] 3. The "gaps" of the inverted-V structure, ~7–10 km in width at 100 km altitude, were colocated with small-scale, downward field-aligned currents.

[23] 4. The field-aligned electric field intensity observed by FAST was rather weak and stable (from zero to less than −10 mV/m) in both the pulsation 1 and pulsation 2 regions, which suggests that the acceleration region might be located far from the FAST satellite altitude.

[24] 5. Both the optical emission intensity at Syowa and the downgoing high-energy electron flux (>7 keV) onboard FAST show ~3 Hz modulation. This ~3 Hz modulated fine structure constitutes the main body of the ~6 s pulsating aurora. The form of the ~3 Hz optical pulsating aurora occurs along the east-west aligned ~6 s pulsating auroral form although each east-west aligned ~3 Hz filament is narrow in the north-south direction in comparison to the main body of the ~6 s pulsating aurora.

[25] 6. The downgoing ~3 Hz modulated electrons exhibited energy-time dispersion. Using this time lag, the source regions of the generation/modulation of energetic particles are calculated to be ~2 Re to 6 Re from the FAST satellite along the field line. The ~6 s pulsation "OFF" signature showed the same energy dispersion and time lag as that of the ~3 Hz modulation.

[26] 7. These results suggest that the source region of the quasi-periodic modulations (~6 s and ~3 Hz) and the resulting electron precipitation is not located in the equatorial plane of the magnetosphere but is located earthward, far from the equatorial plane.

[27] 8. While FAST was traversing the region over Syowa, interhemispheric differences in the shape of the pulsating auroral form, determined using the Syowa-Iceland conjugate pair, were apparent. Although pulsating aurora was observed in both hemispheres, an east-west aligned band was observed in the Southern Hemisphere, while a torch structure (omega band) was present in the Northern Hemisphere.

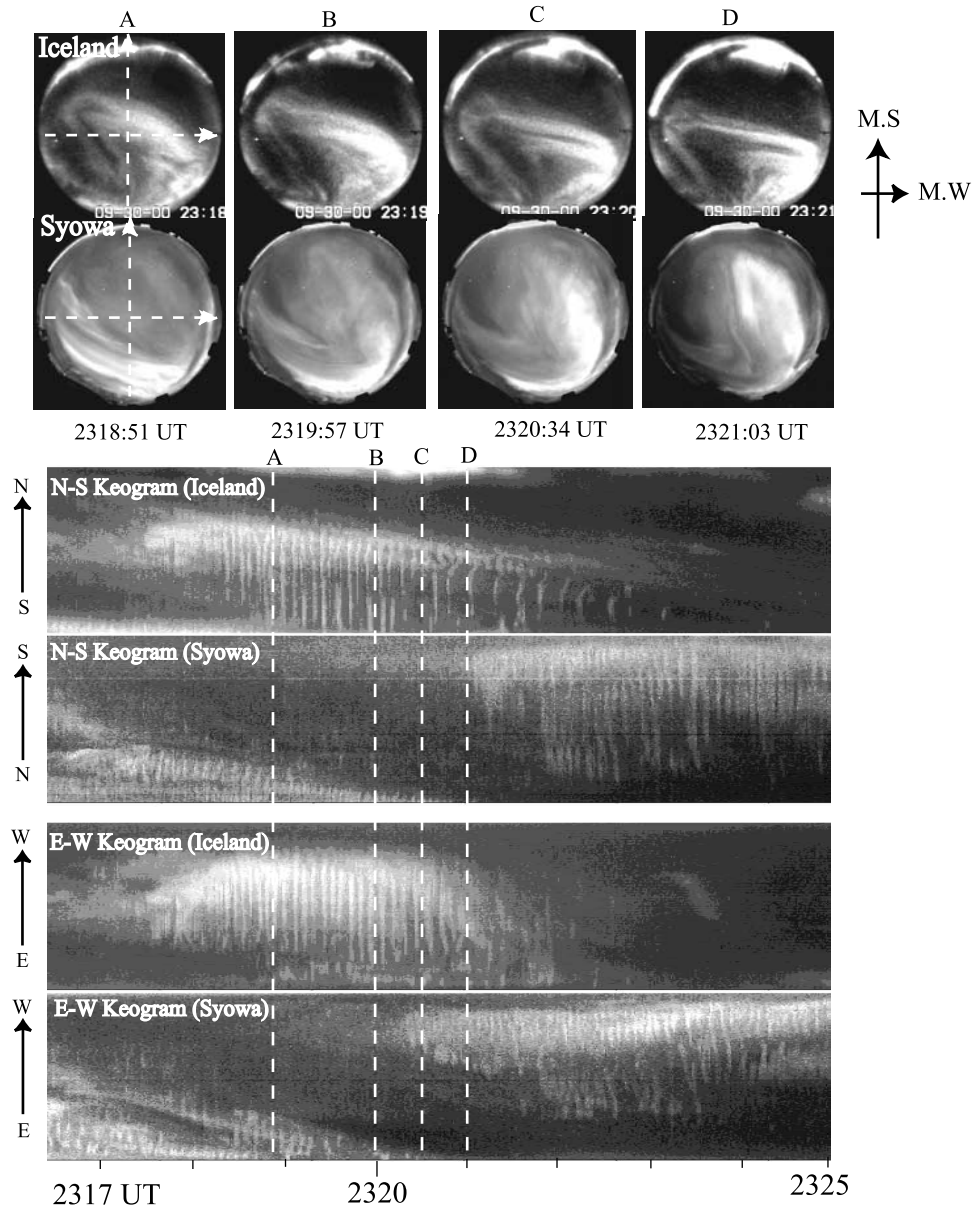

Figure 8. The top panel shows snapshot images from the conjugate pair of all-sky cameras obtained at 2318:31 UT, 2318:51 UT, and 2319:11 UT. The middle two panels and the bottom two panels show the conjugate Keograms reproduced from the all-sky TV camera data in the directions of geomagnetic north-south and east-west, respectively. The positions and directions for each Keogram are marked on the snapshot displays of the all-sky images in the top left panel. The vertical dotted lines in the Keograms show the times of the snapshot auroral images displayed in the top panel of this figure.

[28] 9. A torch structure pulsating aurora at Syowa appeared ~3 min later than a similar type of pulsating aurora occurred in Iceland. There were interhemispheric discrepancies in the shape of the torch structure aurora and the dynamic features of the pulsating aurora.

[29] We shall now discuss the generation region, mechanism, and shape of the pulsating aurora based on the summary documented above and also on the previous report of *Sato et al.* [2002] as documented in section 1. A schematic model to explain this event is shown in Figure 9, which illustrates the modulation region of the pulsating auroras and the generation of the shape of the observed aurora. The form of the east-west aligned multiband aurora reported in this study showed a clear relationship, with the inverted-V structure of the 0.1–1 keV downgoing electrons. This signature is very similar to those of east-west aligned discrete arcs, although the peak energy for a discrete arc is typically a few keV to 10 keV. Another interesting point drawn from this study is that there are two different types of pulsating aurora, which are clearly separated by the "gap" in the inverted-V structure. These features suggest that the form of east-west aligned band-type pulsating aurora may be related to the inverted-V potential structure because of the analogy to the shaping of east-west aligned discrete

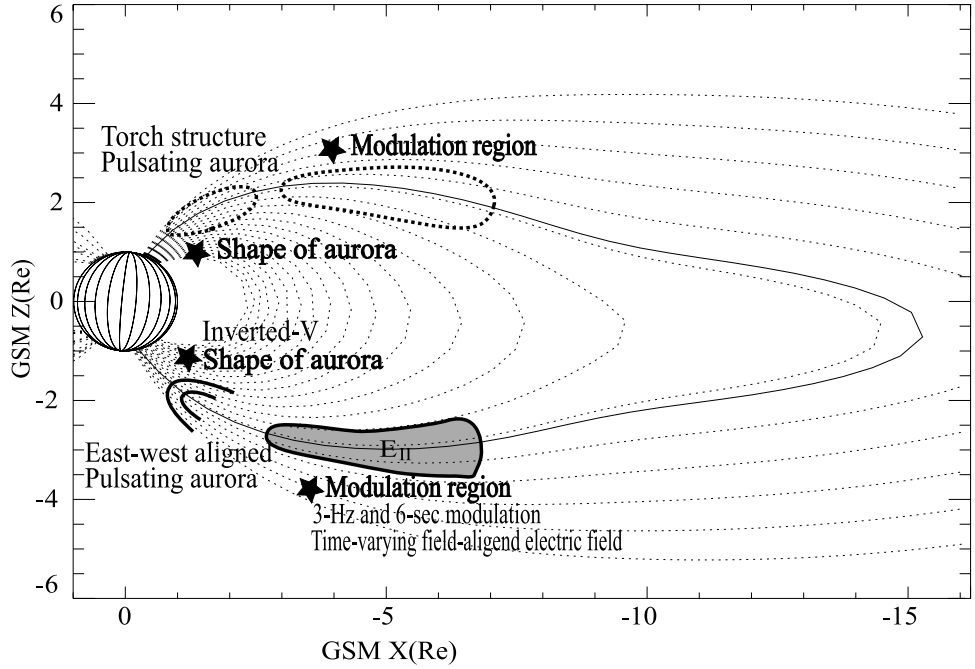

Figure 9. Schematic model to illustrate the generation of the shape of the observed aurora and the location of the modulation region of the auroral pulsations. The quasi-static potential structure, which is generating the inverted-V structure in electron precipitation, may contribute to form the east-west aligned band configuration.

auroral arcs, which is now widely accepted. The inverted-V structure is generally understood to be created typically at altitudes of 5000 to 10,000 km from the Earth's surface by ionosphere-magnetosphere coupling processes. Nonconjugate features of such phenomena would be expected as a result of different geophysical conditions in each hemisphere, especially differences in the conductivity between ionospheric regions [*Newell et al.*, 1996; *Sato et al.*, 1998b]. From this analogy we can also infer that the torch structure form of aurora is created via different spatial form of inverted-V potential structures in the Northern Hemisphere. However, it is found that after the gap "D-E" in the spectrogram/Keogram (top two panels of Figure 2) the inverted-V structure appears to continue, although the >5 keV flux is diminished and FAST is outside of region P-2. This feature suggests that the existence of an inverted-V structure may not be a sufficient condition for producing a pulsating aurora.

[30] The observation that the time-varying downgoing high-energy ion flux modulation was almost out of phase (anticorrelated) with the downgoing, high-energy electron flux modulation [*Sato et al.*, 2002] may be explained by assuming that the precipitating high-energy electrons, which produce the pulsating aurora, are modulated by the time-varying oscillation of the field-aligned electric field located above the FAST satellite. The fact that the time-varying magnetic variation (upward field-aligned current) is almost in phase with the downgoing high-energy electron flux modulation supports this assumption. The current direction is consistent with the electron/ion flux modulation if we assume that the magnetic field variation is the representative for the time-varying field-aligned electric field. However, the precipitating high-energy electrons did not show a sharp flux peak at a selected energy range, such as an inverted-V structure, for either P-1 or P-2. It is possible therefore that the precipitation is not caused directly by parallel acceleration, which energizes the electrons to more than 5 keV, but is due to some other unknown mechanism. In order to solve this problem, a direct observation in a generation/modulation region would be highly desirable.

[31] The mechanism producing the shape of the ~3 Hz pulsation may be closely related to that of the ~6 s pulsation because the ~3 Hz pulsation composes the main body of ~6 s pulsation and the form/shape of both pulsations (east-west aligned aurora) is very similar as documented here. In order to determine the validity of our model, further experimental studies in the source region and further theoretical works are required.

[32] The identification of the source region of the pulsating particle modulation is very important when considering the generation mechanism/theory of pulsating aurora. In this study we found that the source regions of the particle modulation are scattered at the distance ranging between 2.2 Re (~14,100 km) and 6.2 Re (~39,500 km) from FAST along the field line, which means that the source region is located in the region from ~17,200 km to ~42,600 km from the Earth's surface. The latest magnetospheric model suggests that the source region of the quasi-periodic modulation of precipitating electrons is not located in the equatorial plane of the magnetosphere but is located far from the equator, as stated earlier.

[33] Similar source estimation using the energy dispersion technique has previously been employed using rocket experiments. *Lepine et al.* [1980] reported that the source

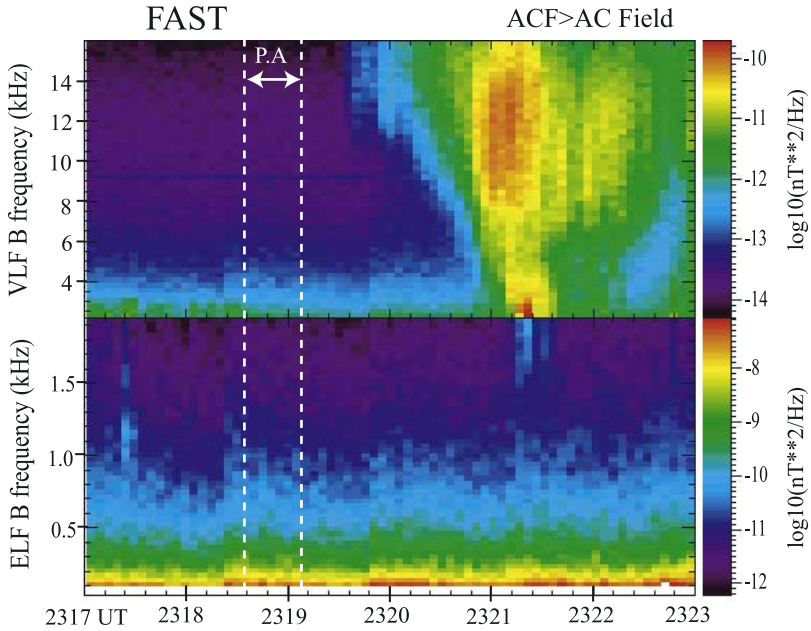

Figure 10. Frequency-time spectra of VLF (upper panel) and ELF (bottom panel) wave activity obtained by FAST. Almost no ELF/VLF wave activity was seen inside the region of the pulsating aurora, though intense auroral hiss emissions were observed in the region of a discrete aurora during the interval of ~2320:30–2322:20 UT.

distance of ~3 Hz modulated high-energy electrons was ~42,000 km from rockets launched from Kiruna, Sweden (L ~ 5.5), and they suggested that the modulation region corresponds to the equatorial region in the dipole field approximation. On the other hand, *Bryant et al.* [1975] calculated the source distance for 1–20 s pulsations obtained over Kiruna and found that the distance varied from 40,000 km to 90,000 km even during the course of a single rocket flight. *Yau et al.* [1981] reported that the calculated modulation region of a 17 s pulsation lay between 43,000 km and 50,000 km using a rocket over Saskatchewan, Canada (L ~ 6). *Smith et al.* [1980] reported that the source distance of a 12 s pulsation was located at ~57,000 km as detected at Andoya, Norway (L ~ 6.4). These rockets flights and our FAST satellite experiments suggest that the location of the source region may vary case by case. The present study appears to give a lower altitude than those obtained in the earlier rocket experiments.

[34] Simultaneous direct observations between geostationary satellites and the ground or rockets could offer a very important opportunity to further investigate the generation mechanism of the classical model/theory. However, such simultaneous observations have been very limited in the past. Only two papers, *Lepine et al.* [1980] and *Nemzek et al.* [1995], have been published to our knowledge. *Lepine et al.* [1980] examined the experimental data obtained by the geostationary GEOS 2 satellite and a rocket geomagnetically conjugate to the satellite. They found that ~3 Hz modulated high-energy electron precipitation detected by the rocket showed a very clear correlation with the 500 Hz VLF wave intensities found by the GEOS 2 satellite. However, GEOS 2 did not detect ~3 Hz pulsations in particle flux variations. Furthermore, they suggested that the variations in pitch angle scattering were not the dominant feature controlling the oscillations because of the isotropic angular distributions of energetic electrons measured by the rocket. This result is at variance with the classical/standard models. *Nemzek et al.* [1995] examined measurements of electron flux and plasma densities at the geosynchronous orbit during times of pulsating auroral activity detected by conjugate all-sky recordings. They found that pulsating auroras are linked to substorm-injected electrons but were unable to find any clear dependence between the plasma density and the pulsations because available measurements of the plasma density variations were too limited. Therefore the two reports discussed above suggest that there is no direct evidence to support the classical/standard model based on observations near the equatorial plane in the magnetosphere, where the generation region is assumed to be located according to the classical/standard models.

[35] Our conclusion, that the source region is located far from the equatorial plane in the magnetosphere, gives a very reasonable explanation of the nonconjugacy of pulsating aurora. Under these conditions, energetic electrons and plasma waves cannot maintain a stable bouncing motion between the conjugate hemispheres. Furthermore, as seen in Figure 10, FAST did not detect any ELF/VLF wave activity inside the region of pulsating aurora, though intense auroral hiss emissions were observed in the region of discrete aurora during the interval of ~2320:30–2322:20 UT. The observations presented here along with those of the other authors stated above [e.g., *Lepine et al.*, 1980] indicate that the generation mechanism and associated source region of pulsating aurora cannot be explained by the classical/standard model. To date, almost all theoretical work

[e.g., *Johnstone*, 1983; *Davidson*, 1990; *Demekhov and Trakhtengerts*, 1994] attempting to explain pulsating aurora has been based on the assumption that the precipitating electrons are produced by pitch angle scattering through wave-particle interactions in the equatorial region of the magnetosphere and that aurora-producing particles precipitate symmetrically into both hemispheres along the geomagnetic field lines. This classical/standard model assumes basically that the energetic particles and the plasma waves perform a stable bouncing motion between the conjugate hemispheres. If so, (1) the pulsating aurora should show a north-south conjugacy, and (2) some VLF electromagnetic wave activity should be evident. However, this study does not support any such hypothesis.

[36] The standard model was, after all, based on observational data, mostly for a patch-type pulsating aurora, as well as theoretical developments. On the other hand, this study is limited to east-west aligned band/arc type pulsations, which is a subset of the entire pulsating aurora phenomenon. Therefore it may well be that there are two (or more) mechanisms at work under different circumstances, although the fundamental ON-OFF feature of the east-west aligned pulsation in this study is analogically the same as that of a patch-type pulsating aurora in terms of the period and the flux modulation ratio. On the other hand, the 3-Hz phenomenon seems to be common to most pulsating aurora displays including midlatitude (subauroral zone) aurora [*Winckler and Nemzek*, 1993], so that this may well be due to a fundamental interaction.

4. Conclusion

[37] The results presented here provide a new insight into the mechanisms that generate pulsating aurora and give a reasonable explanation of its nonconjugate features. The five main conclusions are the following: (1) The source region was located earthward, far from the equatorial plane, (2) the downgoing, high-energy ion flux modulation was almost out of phase (anticorrelated) with the downgoing high-energy electron flux, (3) the magnetic field variation was almost correlated (in-phase) with the down-going high electron flux modulations, (4) the form of the pulsating aurora appeared to be closely related to the inverted-V potential structure, and (5) the pulsating aurora was not conjugate in shape. These findings suggest that ionosphere-magnetosphere coupling processes are important for producing pulsating aurora as previously pointed out by *Stenbaek-Nielsen* [1980] and *Sato et al.* [1998a].

[38] Theoretical and simulation studies are needed to explain the generation of the ~3 Hz pulsation within the main body of the ~6 s pulsation of energetic electrons, which are affected by time-varying oscillations of field-aligned electric fields in regions far from the equatorial plane of the magnetosphere. This is a key issue that must be addressed in order to solve the generation mechanism of pulsating aurora. Simultaneous coordinated observations using satellites that are located in different regions (such as the equatorial plane and middle and low altitudes), rockets, and conjugate pairs of ground observatories are required to answer the key questions regarding the generation region and the generation/modulation mechanisms of pulsating aurora.

[39] **Acknowledgments.** This research was supported by the Grant-in Aid for Scientific Research (A: 11304029 and B: 13573007) from the Japan Society for the Promotion of Science (JSPS). The analysis of FAST data was supported by NASA grant NAG5-3596. The 41st Japanese Antarctic Research Expedition carried out the optical operation at Syowa. K. Tsunezawa assisted with the analysis of the auroral data. R. Strangeway at UCLA provided the FAST magnetic field data for this study. The IMF and solar wind data were obtained from NASA/NSSDC/CDAWeb and provided by Ronald P. Lepping and Keith W. Ogilvie. We would also like to thank A. Kadokura and H. Miyaoka for helpful discussions.

[40] Arthur Richmond thanks Robert J. Nemzek and V. R. Tagirov for their assistance in evaluating this paper.

References

Bryant, D. A., M. J. Smith, and G.-M. Courtier (1975), Distant modulation of electron intensity during the expansion phase of an auroral substorm, *Planet. Space Sci.*, *23*, 867–878.

Carlson, C. W., R. F. Pfaff, and J. G. Watzin (1998), The Fast Auroral Snapshot (FAST) mission, *Geophys. Res. Lett.*, *25*, 2013–2016.

Cash, S. R., J. A. Davies, E. Kolesnikova, T. R. Robinson, D. M. Wright, T. K. Yeoman, and R. J. Strangeway (2002), Modelling electron acceleration within the IAR during a 3Hz modulated EISCAT heater experiment and comparison with FAST satellite electron flux data, *Ann. Geophys.*, *20*, 1499–1507.

Davidson, G. T. (1990), Pitch angle diffusion and the origin of temporal and spatial structures in pulsating aurorae, *Space Sci. Rev.*, *53*, 45–82.

Demekhov, A. G., and V. Y. Trakhtengerts (1994), A mechanism of formation of pulsating aurora, *J. Geophys. Res.*, *99*, 5831–5841.

Harang, L. (1951), *The Aurorae*, Chapman and Hall, New York.

Johnstone, A. D. (1983), The mechanism of pulsating aurora, *Ann. Geophys.*, *1*, 397–410.

Lepine, D. R., D. A. Bryant, and D. S. Hall (1980), A 2.2-Hz modulation of auroral electrons imposed at the geomagnetic equator, *Nature*, *286*, 469–471.

McEwen, D. J., E. Yee, B. A. Whalen, and A. W. Yau (1981), Electron energy measurements in pulsating auroras, *Can. J. Phys.*, *59*, 1106–1115.

Minatoya, H., T. Ono, N. Sato, K. Makita, and T. Yoshino (1994), Development of image data processing system for the conjugate auroral TV data, *Antarct. Rec.*, *38*, 113–147.

Nemzek, R. J., R. Nakamura, D. N. Baker, R. D. Belian, D. J. McComas, M. R. Thomsen, and T. Yamamoto (1995), The relationship between pulsating auroras observed from the ground and energetic electrons and plasma density measured at geosynchronous orbit, *J. Geophys. Res.*, *100*, 23,935–23,944.

Newell, P. T., C.-I. Meng, and K. M. Lyon (1996), Suppression of discrete aurorae by sunlight, *Nature*, *381*, 766–767.

Oguti, T. (1978), Observations of rapid auroral fluctuations, *J. Geomagn. Geoelectr.*, *30*, 299–314.

Oguti, T., S. Kokubun, K. Hayashi, K. Tsuruda, S. Machida, T. Kitamura, O. Saka, and T. Watanabe (1981), An auroral torch structure as an activity center of pulsating aurora, *Can. J. Phys.*, *59*, 1056–1062.

Royrvik, O., and T. N. Davis (1977), Pulsating aurora: Local and global morphology, *J. Geophys. Res.*, *82*, 4720–4740.

Sandahl, I., L. Eliasson, and R. Lundin (1980), Rocket observations of precipitating electrons over a pulsating aurora, *Geophys. Res. Lett.*, *7*, 309–312.

Sato, N., M. Morooka, H. Minatoya, and T. Saemundsson (1998a), Nonconjugacy of pulsating auroral patches near L = 6, *Geophys. Res. Lett.*, *25*, 3755–3758.

Sato, N., T. Nagaoka, K. Hashimoto, and T. Saemundsson (1998b), Conjugacy of isolated auroral arcs and nonconjugate auroral breakups, *J. Geophy. Res.*, *103*, 11,641–11,652.

Sato, N., D. M. Wright, Y. Ebihara, M. Sato, Y. Murata, H. Doi, T. Saemundsson, S. E. Milan, M. Lester, and C. W. Carlson (2002), Direct comparison of pulsating aurora observed simultaneously by the FAST satellite and from the ground at Syowa, *Geophys. Res. Lett.*, *29*(21), 2041, doi:10.1029/2002GL015615.

Smith, M. J., D. A. Bryant, and T. Edwards (1980), Pulsations in auroral electrons and positive ions, *J. Atmos. Terr. Phys.*, *42*, 167–187.

Stenbaek-Nielsen, H. C. (1980), Pulsating aurora: The importance of the ionosphere, *Geophys. Res. Lett.*, *7*, 353–356.

Stenbaek-Nielsen, H. C., T. N. Davis, and N. W. Glass (1972), Relative motion of auroral conjugate points during substorms, *J. Geophys. Res.*, *77*, 1844–1858.

Tagirov, V. R., V. S. Ismagilov, E. E. Titova, V. A. Arinin, A. M. Perlikov, J. Manninen, T. Turunen, and K. Kaila (1999), Auroral pulsations and accompanying VLF emissions, *Ann. Geophys.*, *17*, 66–78.

Trakhtengerts, V. Y., V. R. Tagirov, and S. A. Chernous (1986), A circulating cyclotron maser and pulsed VLF emissions, *Geomagn. Aeron.*, *26*, 77–82.

Tsyganenko, N. A. (2002a), A model of the near magnetosphere with a dawn-dusk asymmetry: 1. Mathematical structure, *J. Geophys. Res.*, *107*(A8), 1179, doi:10.1029/2001JA000219.

Tsyganenko, N. A. (2002b), A model of the near magnetosphere with a dawn-dusk asymmetry: 2. Parameterization and fitting to observations, *J. Geophys. Res.*, *107*(A8), 1176, doi:10.1029/2001JA000220.

Tsyganenko, N. A., H. J. Singer, and J. C. Kasper (2003), Storm-time distortion of the inner magnetosphere: How severe can it get?, *J. Geophys. Res.*, *108*(A5), 1209, doi:10.1029/2002JA009808.

Winckler, J. R., and R. J. Nemzek (1993), Observations of the pulsating phase of auroras observed at Minneapolis during the peak of solar Cycle 22, in *Auroral Plasma Dynamics*, *Geophys. Monogr. Ser.*, vol. 80, edited by R. L. Lysak, pp. 1–15, AGU, Washington, D. C.

Yamamoto, T. (1988), On the temporal fluctuations of pulsating auroral luminosity, *J. Geophys. Res.*, *93*, 897–911.

Yau, A. W., B. A. Vhalen, and D. J. McEven (1981), Rocket-borne measurements of particle pulsation in pulsating aurora, *J. Geophys. Res.*, *98*, 5673–5681.

C. W. Carlson, Space Science Laboratory, University of California, Berkeley, CA 94720-7450, USA. (cwc@ssl.berkeley.edu)

Y. Ebihara, and N. Sato, National Institute of Polar Research, 1-9-10, Kaga, Itabashi-ku, Tokyo, 173-8515, Japan. (ebihara@nipr.ac.jp; nsato@nipr.ac.jp)

M. Lester, S. E. Milan, and D. M. Wright, Department of Physics and Astronomy, University of Leicester, Leicester, LE1 7RH, UK. (mle@ion.le.ac.uk; ets@ion.le.ac.uk; Darren.Wright@ion.le.ac.uk)

T. Saemundsson, Science Institute, University of Iceland, Dunhaga 5, Reykjavik, IS-107, Iceland. (halo@raunvis.hi.is)

M. Sato, Department of Geophysics, Graduate School of Science, Tohoku University, Aramaki, Aoba, Sendai 980-8578, Japan. (mitsu-sato@riken.jp)